Temperature dependences of geometrical and velocity-matching resonances in $Bi_2Sr_2CaCu_2O_{8+x}$ intrinsic Josephson junctions

S. O. Katterwe and V. M. Krasnov

Department of Physics, Stockholm University, AlbaNova University Center, SE-10691 Stockholm, Sweden

(Received 29 July 2011; revised manuscript received 5 December 2011; published 16 December 2011)

We study temperature dependence of geometrical (Fiske) and velocity-matching (Eck) resonances in the flux-flow state of small $Bi_2Sr_2CaCu_2O_{8+x}$ mesa structures. It is shown that the quality factor of resonances is high at low T, but rapidly decreases with increasing temperature. We also study T dependencies of resonant voltages and the speed of electromagnetic waves (the Swihart velocity). Surprisingly it is observed that the Swihart velocity exhibits a flat T dependence at low T, following T dependence of the c-axis critical current, rather than the expected linear T dependence of the London penetration depth. Our data indicate that self-heating is detrimental for operation of mesas as coherent THz oscillators because it limits the emission power via suppression of the quality factor. On the other hand, significant temperature dependence of the Swihart velocity allows broad-range tunability of the output frequency.

DOI: 10.1103/PhysRevB.84.214519 PACS number(s): 74.72.Gh, 74.78.Fk, 74.50.+r, 85.25.Cp

I. INTRODUCTION

Single crystals of a cuprate superconductor $Bi_2Sr_2CaCu_2O_{8+x}$ (Bi-2212) represent natural stacks of atomic scale intrinsic Josephson junctions (IJJs).[1] Josephson junctions form transmission lines for electromagnetic (EM) waves.[2] The propagation (Swihart) velocity is $c_0 \simeq c/[L_\square C_\square]^{1/2}$, where c is the speed of light in vacuum and $L_\square$ and $C_\square$ are the inductance and the capacitance per square of the transmission line,

$$L_\square = 4\pi\Lambda, \tag{1}$$

$$\Lambda = t + 2\lambda_S \coth(d/\lambda_S). \tag{2}$$

Here t and d are thicknesses of the dielectric and superconducting layers, respectively, and λ_S is the London penetration depth of the superconductor. In thin-layer junctions $t,d \ll \lambda_S$, $L_\square \simeq 8\pi\lambda_S^2/d$ is dominated by a large kinetic inductance of superconducting layers. As a consequence, c_0 can be much slower than c—the phenomenon that finds applications in compact superconducting delay lines.[3]

The Swihart velocity carries a direct information about the London penetration depth. It can be obtained by measuring the propagation (delay) time in a transmission line.[4,5] However, Josephson junctions provide a much easier way of measuring c_0. In Josephson junctions EM waves can be generated *in situ* by means of the ac-Josephson effect. At geometrical resonance conditions they form standing waves, leading to the appearance of Fiske steps in current-voltage (I-V) characteristics.[6–10] Fiske step voltages allow simple and direct evaluation of the *absolute values* of temperature-dependent London penetration depth[2,6,11] (unlike surface impedance measurements, which usually provide only relative values[12–15]). Such measurements do not require long transmission lines, but can be performed on small $\sim\mu$m-scale junctions. IJJs of μm sizes, made on high quality Bi-2212 single crystals, are free from crystallographic defects that can affect λ in cuprates.[16,17] Therefore Fiske resonances in small IJJs should provide information about genuine (defect-free) behavior of the penetration depth in cuprates.

Geometrical resonances play also an important role in achieving high power THz EM wave emission from Bi-2212 mesa structures.[18–23] The maximum radiation power from a stack with N junctions is $P_{\rm rad} \propto N^2Q^2$,[24] where

$$Q = \omega RC \tag{3}$$

is the quality factor of the resonance, ω is the resonant frequency, R is the effective damping resistance, and C is the capacitance of the junctions. The factor N^2 is due to constructive interference of N in-phase synchronized junctions[25] and the factor Q^2 represents the resonant amplification in each junction by the geometrical resonance. Thus both in-phase coherence and high quality $Q \gg 1$ geometrical resonances are needed for achieving a high emission power.[24] The increment of the emission power is inevitably accompanied by self-heating of the stack. In superconductors this leads to a rapid increase of the quasiparticle (QP) damping, which suppresses Q. Self-heating ultimately limits the performance of an oscillator.[23] Clearly, investigation of the quality factor of geometrical resonances and their T dependence has a primary significance for the development of a high power THz oscillator, based on IJJs.

In this work, we study experimentally T dependencies of geometrical (Fiske) and velocity-matching (Eck) resonances[9] in the flux-flow state of small Bi-2212 mesa structures. It is observed that Q of resonances is large at low T, but rapidly decreases with increasing temperature primarily due to enhancement of the quasiparticle damping. Surprisingly, it is observed that resonant voltages, proportional to the Swihart velocity, exhibit a very weak T dependence at low T and do not follow the expected linear T dependence of the effective London penetration depth $\lambda_{ab}(T)$ in Bi-2212.[12–15] We discuss possible origins of such a distinct discrepancy, which to our opinion deserves further experimental and theoretical analysis.

II. GEOMETRICAL RESONANCES IN STACKED JOSEPHSON JUNCTIONS

Stacked Josephson junctions form multilayer transmission lines for electromagnetic waves. The general problem of linear

wave propagation in multilayer transmission lines was first considered by Economou[26] and more recently within the inductively coupled junction (ICJ) formalism by Kleiner[27] and Sakai *et al.*[28] In this section we will briefly recollect peculiarities of wave propagation and geometrical resonances in stacked Josephson junctions.

In the ICJ model of Sakai, Bodin, and Pedersen,[29] a layered superconductor is represented by a stack of isotropic superconducting layers with the thickness d and the "intrinsic" penetration depth λ_S, separated by tunnel barriers with the thickness t, the dielectric constant ϵ_r, and the fluctuation-free Josephson critical current density at zero magnetic field J_{c0}. The stacking periodicity $s = t + d$ is $\simeq 1.5$ nm for Bi-2212. Properties of inductively coupled stacked Josephson junctions are described by the coupled sine-Gordon equation.[29] The coupling is represented by a tridiagonal coupling matrix A with the off-diagonal terms equal to minus the effective inductive coupling constant between neighbor junctions,[28]

$$S = \lambda_S \left[t \sinh\left(\frac{d}{\lambda_S}\right) + 2\lambda_S \cosh\left(\frac{d}{\lambda_S}\right)\right]^{-1}. \quad (4)$$

For IJJs $S \simeq 0.5 - ds/4\lambda_S^2$ is close to the maximum value 0.5.

A. Eigenmodes in stacked junctions

The main difference between single and stacked junctions is the presence of multiple electromagnetic wave modes in the stack. Geometrical resonances in a stack correspond to formation of two-dimensional standing waves.[27,28] The wave number along the ab planes (x axis) is $k_m = \pi m/L$, where L is the length of the junctions and m is the number of nodes in the standing wave. In the c-axis direction it is given by one of the eigenmodes, $k_n = \pi n/(N+1)s$, $n = 1,2,\ldots N$, where N is the number of junctions in the stack. The oscillatory part of the phase difference is

$$\delta\varphi_i(m,n) = a\cos\left(\frac{\pi m x}{L}\right)\sin\left(\frac{\pi n i}{N+1}\right)e^{j\omega t}. \quad (5)$$

Here $i = 1,2,\ldots N$ is the junction index, $a = \text{const}$ is an amplitude, and ω is the angular frequency.

Each eigenmode has a distinct propagation velocity, given by Eq. (3.52) of Ref. 26. Within the ICJ model they can be written as[28]

$$c_n = c_0\left[1 - 2S\cos\left(\frac{\pi n}{N+1}\right)\right]^{-1/2}, \quad n = 1,2,\ldots N, \quad (6)$$

where $c_0 = \lambda_J\omega_{p0} = c[ts/2\epsilon_r\lambda_{ab}^2]^{1/2}$ is the Swihart velocity,

$$\omega_{p0} = \left[\frac{8\pi^2 tcJ_{c0}}{\Phi_0\epsilon_r}\right]^{1/2} \quad (7)$$

is the Josephson plasma frequency (at zero magnetic field),

$$\lambda_J = \left[\frac{\Phi_0 c}{8\pi^2 J_{c0}\Lambda}\right]^{1/2} \simeq \left[\frac{\Phi_0 cs}{16\pi^2 J_{c0}\lambda_{ab}^2}\right]^{1/2} \quad (8)$$

is the Josephson penetration depth of a single junction, and

$$\lambda_{ab} \simeq \lambda_S\sqrt{s/d} \quad (9)$$

is the effective London penetration depth for field perpendicular to layers.

Similarly, eigenmodes are characterized by different characteristic lengths,[30]

$$\lambda_n = \lambda_J\left[1 - 2S\cos\left(\frac{\pi m}{N+1}\right)\right]^{-1/2}, \quad n = 1,2,\ldots N. \quad (10)$$

$(\lambda_J/\lambda_n)^2$ are eigenvalues of the coupling matrix A.[30] The shortest, $\lambda_N \simeq \lambda_J/\sqrt{2} \simeq 0.5$ μm for Bi-2212. The longest λ_1 approaches the effective penetration depth for field parallel to layers (for $N \gg \pi\lambda_{ab}/s \simeq 400$)

$$\lambda_c = \left[\frac{\Phi_0 c}{8\pi^2 J_{c0} s}\right]^{1/2}. \quad (11)$$

In Bi-2212, $\lambda_c(T=0) \sim 100$ μm $\gg \lambda_{ab}(T=0) \simeq 0.2$ μm.[30]

Due to inductive coupling between junctions, the in-plane (y-axis) magnetic field is nonlocal and depends on phase distributions in all junctions: $B_y(i) = (H_0/2)A^{-1}\lambda_J\partial\varphi_j/\partial x$. Here $H_0 = \Phi_0/\pi\lambda_J\Lambda$.[30] Using Eq. (5) we obtain for the oscillatory part of magnetic field in the stack

$$B_y(x,z)(m,n) = -\frac{H_0 a\pi m\lambda_n^2}{2L\lambda_J}\sin(k_m x)\sin(k_n z). \quad (12)$$

Here we used the property that A and A^{-1} have the same eigenvectors, and eigenvalues of A^{-1} are λ_n^2/λ_J^2, Eq. (10).

The in-plane current density in superconducting layers is obtained from the Maxwell equation $J_x = -(c/4\pi)\partial B_y/\partial z$:

$$J_x(x,z)(m,n) = J_{ac}(m,n)\sin(k_m x)\cos(k_n z), \quad (13)$$

$$J_{ac}(m,n) = \frac{a\Phi_0 c\lambda_n^2 mn}{16\lambda_{ab}^2\lambda_J L(N+1)}. \quad (14)$$

Figure 1 shows calculated distributions of the amplitudes of B_y (a) and J_x (b) for modes $n = N$ (open circles) and $n = 1$ (squares) for the stack with $N = 10$ junctions. Horizontal stripes represent superconducting layers. It is seen that eigenmodes are characterized by different symmetries along

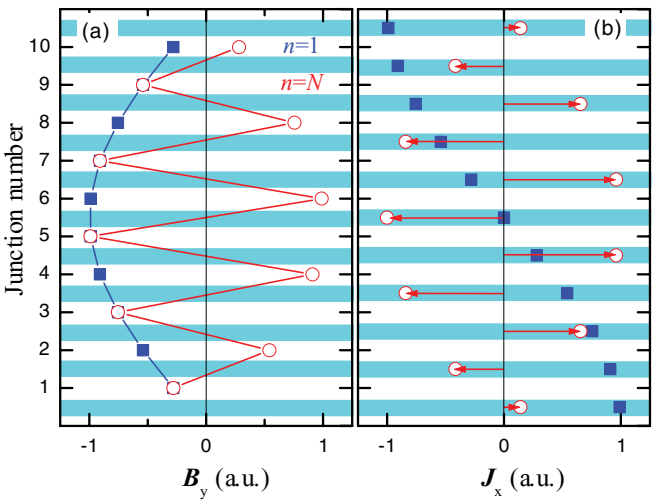

FIG. 1. (Color online) Spatial distribution of oscillation amplitudes of (a) magnetic field and (b) in-plane currents for the in-phase (squares) and the out-of-phase (circles) modes for a stack with $N = 10$ IJJs. Horizontal stripes represent superconducting layers.

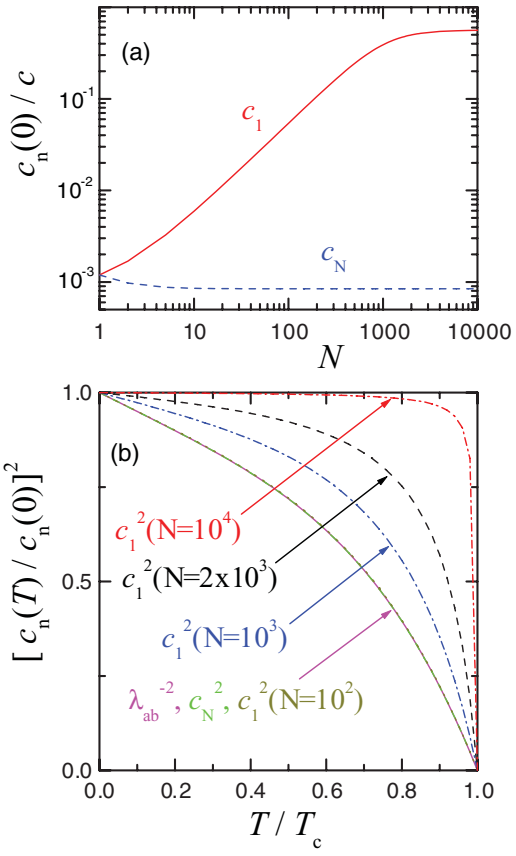

FIG. 2. (Color online) (a) Calculated slowest and fastest velocities c_N and c_1 as a function of the number of junctions in the stack. Calculations are made within the ICJ model for typical Bi-2212 parameters at $T = 0$. (b) Calculated temperature dependencies of squares of c_N and c_1 for several N along with $\lambda_{ab}^{-2}(T)$, normalized by the corresponding values at $T = 0$.

the stacking direction. The slowest $n = N$ mode corresponds to the (almost) out-of-phase state in neighbor junctions $\delta\varphi_i \simeq -\delta\varphi_{i+1}$. The fastest $n = 1$ mode corresponds to the (almost) in-phase state $\delta\varphi_i \simeq \delta\varphi_{i+1}$.

Figure 2(a) shows calculated dependence of c_1 and c_N on the number of junctions N. It is seen that the slowest velocity is almost independent of N,[10]

$$c_N \simeq \frac{c_0}{\sqrt{2}} \simeq c\left[\frac{ts}{4\epsilon_r\lambda_{ab}^2}\right]^{1/2}. \tag{15}$$

To the contrary, the fastest velocity

$$c_1 \simeq c\sqrt{\frac{t}{\epsilon_r s}}\left[1+\left(\frac{\pi\lambda_{ab}}{s(N+1)}\right)^2\right]^{-1/2} \tag{16}$$

is growing linearly with N for $N < \pi\lambda_{ab}/s \simeq 400$.[10] For $N \gg \pi\lambda_{ab}(T)/s$, it asymptotically approaches the T-independent value $c_1(N\to\infty) = c[t/\epsilon_r s]^{1/2}$, close to the speed of light in the dielectric, as shown in Fig. 2(a).

Figure 2(b) shows calculated T dependencies of c_1^2 and c_N^2, Eq. (6), normalized on the corresponding values at $T = 0$, for different N. Calculations are made for typical parameters of Bi-2212, using the $[\lambda_{ab}(T)/\lambda_{ab}(0)]^{-2}$ dependence shown by the lowest line obtained from surface impedance measurements.[12–15,17] As follows from Eq. (15), T dependence of the out-of-phase velocity c_N follows $1/\lambda_{ab}(T)$, irrespective of N. For IJJs the same is true for all slow modes $n \geqslant 2$.

The speed of the fastest mode, $c_1(T)$, does depends on N. For $N < \pi\lambda_{ab}/s \simeq 400$, it maintains the same T dependence $\propto 1/\lambda_{ab}$. The corresponding three curves $[c_N(T)/c_N(0)]^2$, $[\lambda_{ab}(T)/\lambda_{ab}(0)]^{-2}$, and $[c_1(T)/c_1(0)]^2$ for $N = 100$ collapse in one in Fig. 2(b). For much larger N, when c_1 approaches the T-independent speed of light in the dielectrics, see Fig. 2(a), $c_1(T)$ becomes flatter at low T, as shown in Fig. 2(b). However, since λ_{ab} diverges at $T \to T_c$, c_1 always vanishes at T_c, as seen from the curve with $N = 10^4$ in Fig. 2(a).

In magnetic field H, parallel to the junction plane, Josephson vortices (fluxons)[30] enter into the junctions. In strong enough magnetic field fluxons form a regular fluxon lattice in a stack. Usually a triangular lattice is most stable due to fluxon repulsion. However, a rectangular lattice can be stabilized via geometrical confinement in small Bi-2212 mesas.[31] Motion of fluxons leads to appearance of the flux-flow (FF) branch in the I-V. Emission of EM waves in the FF state leads to excitation of geometrical resonances.[7,9,10] The corresponding Fiske step voltage for the resonant mode (m,n) is

$$V_{m,n}(T) = \Phi_0 m c_n(T)/2L. \tag{17}$$

The strongest resonance occurs at the velocity matching (VM) condition, when the velocity of fluxons is equal to the velocity of electromagnetic waves.[10] This leads to the appearance of the VM (Eck) step at the end of the FF branch.[9] The VM voltage is

$$V_{VM} \simeq NHsc_n. \tag{18}$$

The T dependencies of both Fiske and VM steps are determined solely by $c_n(T)$, Eq. (6). Therefore they can be used for accurate detection of the absolute value of $\lambda_{ab}(T)$ [except for the fastest mode at very large N, as shown in Fig. 2(b)].

B. Connection between the inductively coupled and the Lawrence-Doniach models

A similar system of coupled sine-Gordon equations was also obtained from the Lawrence-Doniach (LD) model.[32] The two main parameters of the LD model are the anisotropy factor $\gamma \gg 1$ and the effective London penetration depths λ_{ab}. The rest of parameters are derived as[32] $\lambda_c = \gamma\lambda_{ab}$, $\lambda_J = \gamma s$, $\omega_{p0} = c/\epsilon_r^{1/2}\gamma\lambda_{ab}$, and $c_0 = cs/\epsilon_r^{1/2}\lambda_{ab}$.

From comparison with ICJ expressions Eqs. (7)–(9), (11), and (15) it is seen that while the ICJ model contains two T-dependent variables $\lambda_{ab}(T)$ and $J_{c0}(T)$, the LD model has only one, $\lambda_{ab}(T)$, which imposes its T dependence on all other variables. Within the range of validity of the LD model, $T_c - T \ll T_c$, the two models are identical because $\lambda_{ab}^{-2}(T) \propto J_{c0}(T) \propto 1 - T/T_c$. However, as will be discussed below, $\lambda_{ab}^{-2}(T)$ and $J_{c0}(T)$ have distinctly different T dependencies at low T, which would cause a discrepancy between the two models, unless the anisotropy is allowed to be T dependent, $\gamma(T) = \lambda_c(T)/\lambda_{ab}(T)$.[33–35] Additional discussion about the connection between ICJ and LD models can be found in Ref. 30 (see Table I therein).

III. EXPERIMENT

Small mesa structures were fabricated on top of Bi-2212 single crystals with $T_c = 82$ K. Twelve mesas with different sizes were fabricated simultaneously on every crystal. All of the studied mesas showed similar behavior. Here we present data for two mesas on the same slightly underdoped Bi-2212 crystal with areas of $2.7 \times 1.4\ \mu\text{m}^2$ (mesa 1) and $2.0 \times 1.7\ \mu\text{m}^2$ (mesa 2). Both mesas contain $N = 12$ IJJs. The results are representative for a large number of mesas made on crystals with different doping and composition (see Table I in Ref. 10). Details of sample fabrication and of the experimental setup can be found in Ref. 10.

The magnetic field was applied strictly parallel to the superconducting CuO bilayers, to avoid the intrusion of Abrikosov vortices. Eventual entrance of Abrikosov vortices is immediately obvious in experiment: it causes very strong and irreversible damping of Fiske resonances and of the Fraunhofer modulation of the critical current.[31] Essentially, results reported here are observable only in the absence of Abrikosov vortices. Using the rigorous alignment procedure, described in Ref. 31, we were able to prevent Abrikosov vortex entrance in fields up to 17 T.[36,37] This is seen from the field independence of the c axis QP resistance[36] and perfect reversibility of all measured characteristics.[10,31]

Measurements are made in the three-probe configuration. To simplify data analysis, a contact or a quasiparticle resistance was subtracted from I-V characteristics, as described in Ref. 31. The subtraction is facilitated by the negligible dependence of the QP resistance on in-plane magnetic field due to the extremely large anisotropy of Bi-2212 [see, e.g., Fig. 3(d) in Ref. 36]. To do the subtraction, we first carefully measured the corresponding branch of the I-V at $H = 0$. After that we made a high-order polynomial fit of $\ln(I)$ vs V, which is almost linear[38] and can be fitted with a very high ($\sim\mu$V) accuracy. This fit is then subtracted from the measured I-V. When studying T dependence, this procedure was repeated at each T. Such subtraction simplifies the analysis of Fiske steps, but is not necessary: Fiske steps can be also measured relative to the bias-dependent contact or QP voltages.

IV. RESULTS

Figure 3 shows I-V curves (digital oscillograms) for mesa 1 at $H = 1.4$ T and at different T from 2.0 to 15.1 K. As the current is increased, the I-Vs switch from the zero voltage branch to the flux-flow branch, containing sequences of individual and collective Fiske steps, seen as small subbranches in Fig. 3(a), and ending at the velocity-matching step. Detailed discussion of the magnetic-field dependence of Fiske and VM steps at low T can be found in Ref. 10. Strong hysteresis of Fiske steps indicates high $Q \gg 1$ of the geometric resonances. This is facilitated by careful alignment of magnetic field, which prevents penetration of Abrikosov vortices.[36] With further increase of current some junctions switch into the QP state, while the rest are remaining in the flux-flow state. This leads to the appearance of combined QP-FF families of Fiske steps, four of which are indicated in Fig. 3(a), (QP1–4) with the number corresponding to the number of IJJs in the QP state.

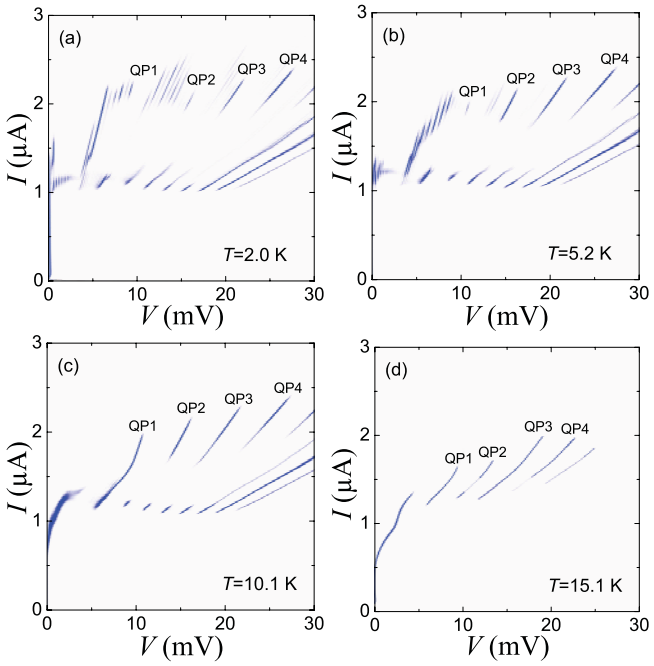

FIG. 3. (Color online) I-V curves of mesa 1 at $H = 1.4$ T and at different $T = 2.0$–15.1 K. At low T, in panels (a) and (b), sequences of hysteretic (high-Q) individual Fiske steps are seen at low bias. At higher bias some junctions switch into the QP state, but Fiske steps are still present in the rest of the junctions. The corresponding first four mixed flux-flow-QP branches are marked (QP1–4). At $T = 10.1$ K (c) these steps smear out and at $T = 15.1$ K (d) individual Fiske steps have vanished; instead a collective, nonhysteretic step is observed.

The EM wave speed can be obtained directly from resonant voltages using Eqs. (17) and (18). The corresponding low-T values for several mesas at different Bi-2212 crystals can be found in Ref. 10. Fiske steps in Fig. 3 correspond to slow speed resonances $V_{2,N} = 0.27$ mV. At the QP1, QP2 branches another sequence $V_{4,N} = 0.54$ mV of individual Fiske steps is seen. As shown in Refs. 10,37, the V_{VM} is proportional to the field for $2\ \text{T} < H < 10$ T, consistent with Eq. (18), before it gets interrupted by phonon-polariton resonances at higher fields.[37] In this intermediate-field range the limiting fluxon velocity is close to the out-of-phase velocity c_N.

A. Temperature dependence of the quality factor

As seen from Fig. 3, with increasing temperature, the amplitude of the individual Fiske steps rapidly decreases. At $T = 10.1$ K steps are smeared out almost completely and at $T = 15.1$ K they vanish. At this temperature only a collective, nonhysteretic Fiske step is visible at $N \times V_{2,N} \simeq 3.2$ mV; see Fig. 3(d).

Figures 4(a) and 4(b) show I-Vs in a wider T range, Fig. 4(a) for mesa 2 at $H = 2.75$ T, and Fig. 4(b) for mesa 1 at $H = 3.85$ T. Collective Fiske steps at $\approx N \times V_{1,N}$ can be seen at low T (indicated by the downward arrows). At higher bias VM steps are observed (indicated by the upward arrows). Both mesas show similar behavior: Sharpness of the collective Fiske and the VM steps rapidly decreases with increasing temperature. This indicates enhancement of damping, also

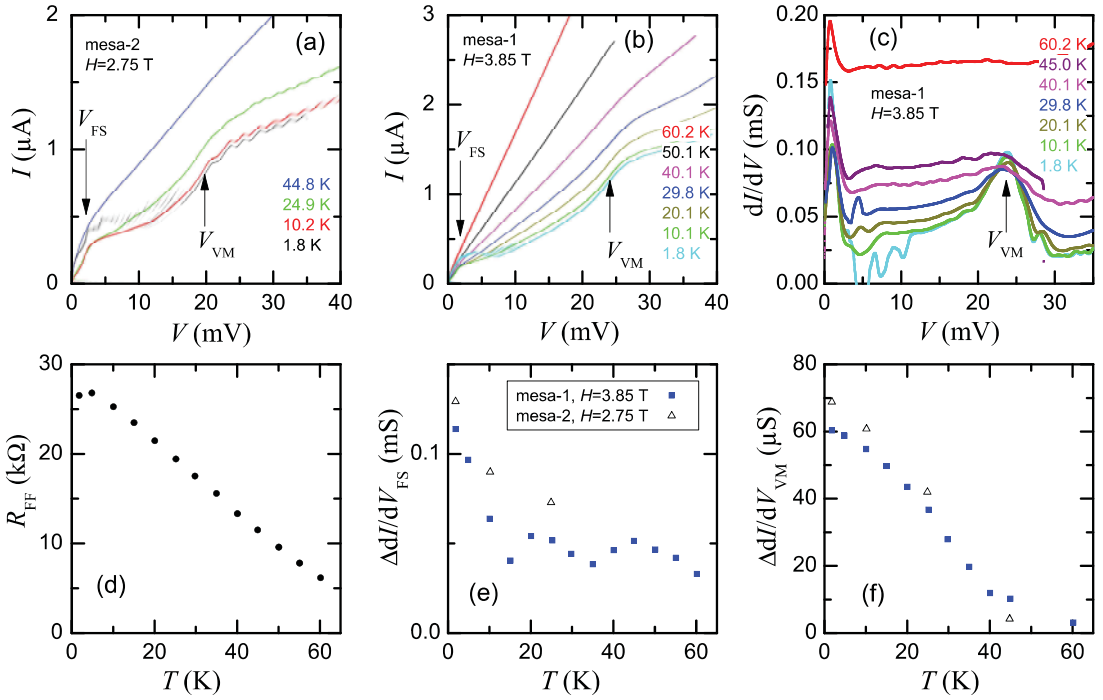

FIG. 4. (Color online) (a) Flux-flow parts of I-V curves of mesa 2 at $H = 2.75$ T and at different T. A collective Fiske step (downward arrow) and a velocity matching step (upward arrow) are seen, followed by QP branches at higher bias $V > 20$ mV. (b) The same for the mesa 1 at $H = 3.85$ T. It is seen that both Fiske and velocity matching steps are rapidly smeared out with increasing T. (c) dI/dV curves, numerically calculated from curves in (b). Distinct peaks correspond to the collective Fiske and the velocity-matching resonances. (d) T dependence of the nearly ohmic flux-flow resistance at $V = 12$ mV for mesa 1 at $H = 3.85$ T. (e) and (f) show amplitudes of the dI/dV peaks, corresponding to the collective Fiske step (e) and the velocity-matching peak (f).

seen from reduction of slopes of I-V curves with increasing T.

Figure 4(c) shows dI/dV curves, numerically calculated from the I-V curves from (b). Peaks in conductance correspond to Fiske and VM steps. The decrease of amplitudes of the steps with increasing T is clearly seen, indicating reduction of Q at higher temperatures.

According to the sine-Gordon equation, the initial viscous part of the flux-flow I-V should be ohmic with the flux-flow resistance R_{FF} representing the effective damping.[39] Indeed, from Figs. 4(a) and 4(b) it is seen that the flux-flow I-V is nearly ohmic at $10 < V < 20$ mV. This allows accurate evaluation of the bare (nonresonant) $R_{FF}(T)$. It is shown in panel (d) for $V = 12$ mV ($\sim$1 mV per junction). The T dependence of R_{FF} is almost identical to the low-bias c-axis QP resistance $R_{QP}(T, H = 0)$,[38] indicating that the $R_{FF}(T)$ dependence is predominantly determined by "freezing out" of quasiparticles. At low T and moderately low H the value of R_{FF} is slightly lower than R_{QP}, which may indicate the presence of additional damping mechanisms, such as the in-plane QP damping,[40] or generation of phonons via electrostriction.[37] At higher H, $R_{FF} = R_{QP}$ [see, e.g., Fig. 3(d) from Ref. 36].

Figures 4(e) and 4(f) represent T dependencies of bare amplitudes of conductance peaks at the collective Fiske step and the VM step, respectively. The peak amplitudes were obtained by subtracting the background flux-flow conductance R_{FF}^{-1}. It is seen that resonances in both mesas exhibit similar T dependencies: At low T, peaks are high, i.e., quality factors of resonances are large $Q \gg 1$, but they start to rapidly decrease with increasing T. Comparison with the effective flux-flow resistance R_{FF}, shown in panel (d), indicates that the scale for variation of peak amplitudes is similar to $R_{FF}(T)$. Therefore both resonances roughly follow Eq. (3) with $R \simeq R_{FF}(T)$.

B. Temperature dependence of the Swihart velocity

Both Fiske and VM steps in the considered case correspond to propagation of waves, respectively fluxons, with the velocity $\simeq 3.2 \times 10^5$ m/s[10] close to the expected value of the slowest out-of-phase velocity c_N, Eq. (15). It is almost 1000 times slower than c, not because of extraordinary large dielectric constant, but because of extraordinary large kinetic inductance of atomically thin superconducting layers in Bi-2212; see Eq. (2). According to Eq. (15), the shape of $c_N(T)$ should depend solely on $1/\lambda_{ab}(T)$. Thus voltages of Fiske and VM steps should provide a direct information on absolute values of $1/\lambda_{ab}(T)$.

Squares and triangles in Fig. 5 represent measured T dependencies of V_{VM}^2 for both studied mesas. Crosses in Fig. 5 represent fast geometrical resonance voltages, reported recently by Benseman and co-workers on large Bi-2212 mesas at zero field.[41] Apparently, our data for the slowest resonances coincide with their data for the fast resonance within the measured T range, consistent with Fig. 2(b) for not very large N.

Lines in Fig. 5 represent typical temperature dependencies of λ_{ab}^{-2} for cuprates[12,13] and the fluctuation-free c-axis critical

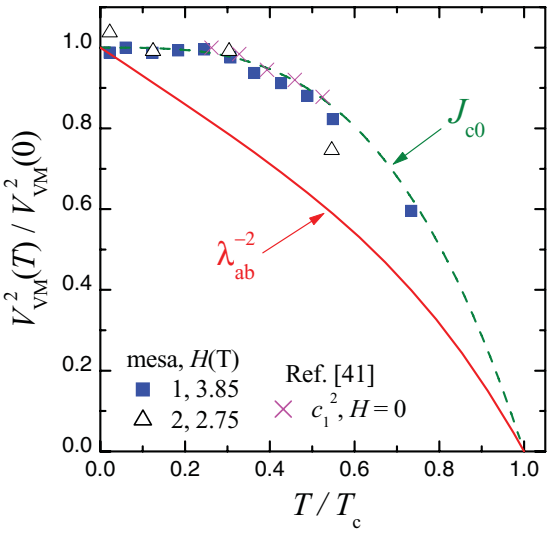

FIG. 5. (Color online) Normalized temperature dependence of the square of the velocity-matching voltage $V_{VM} \propto c_N$. Solid line represents typical T dependence of λ_{ab}^{-2} from Refs. 12 and 13. Dashed line represents the T dependence of the fluctuation free Josephson critical current density J_{c0} from Ref. 42.

current density J_{c0} for Bi-2212 IJJs.[1,42] The latter is similar to $\omega_{p0}^2(T)$, measured by the Josephson plasma resonance[43] and to $\lambda_c^{-2}(T)$ obtained from surface impedance measurements,[34] consistent with Eqs. (7) and (11). It is seen that λ_{ab}^{-2} and J_{c0} exhibit distinctly different behavior at low T: $J_{c0}(T)$ is flat, while $\lambda_{ab}^{-2}(T)$ has a linear T dependence due to the d-wave symmetry of the order parameter.[12,13] Clearly, experimental $V_{VM}^2(T)$ follow $J_{c0}(T)$ rather than the expected $\lambda_{ab}(T)^{-2}$ dependence.

V. DISCUSSION

At low T, the obtained speed of EM waves $\simeq 3.2 \times 10^5$ m/s agrees with the expected out-of-phase mode velocity c_N, Eq. (15) for reasonable parameters $t/\epsilon_r = 0.1$ nm and $\lambda_{ab}(T=0) \simeq 200$ nm,[12,13,15,33] which may correspond, e.g., to $\epsilon_r \simeq 10$, $t \simeq 1$ nm, $d = s - t \simeq 0.5$ nm, and $\lambda_S \simeq 140$ nm. Thus the ICJ model does provide a correct value of the Swihart velocity at low T. It also provides correct T dependencies of the Josephson plasma frequency[43] and λ_c,[34] $\omega_{p0}(T) \propto \lambda_c^{-1}(T) \propto \sqrt{J_{c0}(T)}$; see Eqs. (7) and (11). Therefore it is surprising that the T dependence of the effective penetration depth deduced from resonant voltages is different from $\lambda_{ab}(T)$, obtained from surface impedance measurements.[12,13,15,33] Below we mention several possible reasons for such a discrepancy.

A. Possible origin of discrepancy with surface impedance measurements

It is known that low-T behavior of λ_{ab} in cuprates can be affected by defects and impurities.[17] Especially thin films are prone to such a distortion.[16] However, as we mentioned in the Introduction, here we perform measurements on μm-size mesas made of high quality single crystals. Since such small mesas are free from crystallographic defects, we expect that the corresponding distortion of $\lambda_{ab}(T)$ by defects in our measurements is smaller than in surface impedance measurements performed on much larger crystals. Therefore we discard defects as a possible origin of the discrepancy.

Derivation of the ICJ model is based on the assumption that field and current distributions within each superconducting layer can be described by the local second London equation.[29] However, this assumption most likely breaks down in atomic scale IJJs [see condition (4.3) in Ref. 26].

To understand the reported discrepancy it is, first of all, necessary to understand the difference in local current and field distributions. In surface impedance measurements, the external electromagnetic field is screened at the depth $\lambda_{ab} \sim 200$ nm from the surface of the superconductor. This induces similar (in-phase) screening currents in a fairly large number $N \sim 130$ of IJJs. To the contrary, at the out-of-phase geometrical resonances the current varies at the atomic scale, as shown in Fig. 1(b).

(i) *Nonlocality of supercurrent.* The most obvious question is to what extent Cooper pairs are localized in every CuO bilayer. The very existence of the c-axis critical current indicates that the localization is incomplete. This can be particularly significant for the out-of-phase mode, when Cooper pairs are forced to move in opposite directions in neighbor layers; see Fig. 1(b). Qualitatively such delocalization will lead to larger effective penetration depth.

(ii) *Nonlocal Josephson electrodynamics.* Another type of nonlocality in thin layer junctions was considered by Mints.[44] With decreasing d, the effective screening length $\Lambda/2$, Eq. (3), increases and approaches the Pearl length $\lambda_P = \lambda_S^2/d$. To the contrary, the Josephson penetration depth λ_J decreases $\propto \Lambda^{-1/2}$; see Eq. (8). For IJJs $\lambda_J < 1$ μm Ref. 31 is much smaller than $\lambda_P \sim 10$ μm even at $T = 0$. Such a mismatch changes the dispersion relation of electromagnetic waves.[44]

(iii) *Retardation effects.* Retardation effects appear in transmission lines when the time (phase velocity) required to transfer charge within a layer is comparable or faster than that for electromagnetic waves outside the layer.[26] Specific for IJJs is that the out-of-phase electromagnetic wave velocity is so slow, $\sim 10^5$ m/s, that it becomes comparable to the electronic Fermi velocity. This may affect the dispersion relation.

(iv) *Frequency dependence.* The effective penetration depth in superconductors depends not only on T but also on frequency $\lambda(T,\omega)$. It originates from a significant (T,ω) dependence of complex conductivity in a superconductor.[11] The most obvious difference between static and high-frequency $\lambda(T)$ is that the latter does not diverge at $T \to T_c$, but approaches the finite normal skin depth. This may flatten out T dependence of high-frequency Fiske steps, compared to static $1/\lambda(T)$.[11]

Surface impedance measurements are typically performed at $\sim$10 GHz frequency. In comparison, the studied Fiske and VM step voltages are $\sim$1 mV per junction; see Fig. 4. According to the ac-Josephson relation this corresponds to $\sim$500 GHz. The significant difference in frequencies may lead to a significant difference in the effective λ.

At even higher THz frequencies, the frequency dependence of the dielectric function $\epsilon_r(\omega)$ in isolating BiO layers becomes significant. As shown in Ref. 37, the speed of electromagnetic waves slows down dramatically when the frequency approaches the transverse optical phonon frequencies.

(v) *Nonlinear effects.* Equation (6) was derived by linearization of the coupled sine-Gordon equation and is valid for small amplitude EM waves $a \ll 1$. However, at high quality geometrical resonances the amplitude may be large, $a \sim 2\pi$, and nonlinearity of the sine-Gordon equation may affect the dispersion relation.

The penetration depth depends on the absolute value of the current density. Close to the depairing current density, λ rapidly increases. At geometrical resonances the amplitude of the in-plane current density is given by Eq. (14). It depends on the amplitude a, which can be ~ 1 for $Q \gg 1$. An estimation for $a = 1$ and $L/m = 1$ μm yields $J_{ac} \sim 10^6$ A/cm^2, comparable to the maximum in-plane current density.[45]

Both types of nonlinear effects increase with increasing the quality factor of resonances. Since $Q \gg 1$ only at low T, nonlinear corrections can be significant at low T, but less so at elevated temperatures.

B. Implications for coherent Josephson oscillators

As mentioned in the Introduction, stacked IJJs are considered as possible candidates for high power THz oscillators.[18–23,41] A large energy gap in Bi-2212 (Refs. 36,38) allows generation of electromagnetic radiation with frequencies in excess of 10 THz. For example, recently polariton generation with frequencies up to $\sim$13 THz was reported.[37] Moreover, strong electromagnetic coupling of IJJs facilitates phase locking of many junctions, which may lead to coherent amplification of the emission power.[25]

Realization of a flux-flow oscillator,[7] based on fluxon motion in the in-plane magnetic field,[8,46–48] encounters a difficulty, associated with instability of the rectangular fluxon lattice. It can be stabilized by geometrical confinement in small mesas[31] or by interaction with infrared optical phonons.[37] But usually fluxon-fluxon repulsion promotes the triangular fluxon lattice, corresponding to the out-of-phase state, which leads to destructive interference and negligible emission.[24]

High quality geometrical resonances improve the operation of a stacked oscillator in several ways: (i) they amplify the emission power $\propto Q^2$,[24] (ii) they narrow down the radiation linewidth $\propto 1/Q$,[24] and (iii) they can *force* phase locking of junctions. Numerical simulations have demonstrated that large amplitude standing waves, $a \sim 1$, can superimpose their symmetry on the fluxon lattice.[10] Such a nonlinear synchronization requires high Q because $a \propto Q$.

The reported rapid decrease of the quality factor with increasing temperature indicates that self-heating is detrimental for the coherent Josephson oscillator and ultimately limits the emission power from large Bi-2212 mesas.[23] On the other hand, T dependence of the Swihart velocity facilitates fairly broad-range tuning of the resonance frequency, as seen from Fig. 5. This may be beneficial for the oscillator.[41]

VI. CONCLUSIONS

To conclude, we have studied the T dependence of geometrical and velocity matching resonances in small Bi-2212 mesa structures. We reported a strong T dependence of the quality factors, which is large at low T, but rapidly decreases with increasing T. Above $T \sim 60$ K $\sim 0.8T_c$ resonances are almost fully damped. This observation is consistent with previous observations of strongly underdamped phase dynamics at low T,[42] leading to relatively high macroscopic quantum tunneling temperature in IJJs,[49–51] and with the reported collapse into overdamped dynamics at $T/T_c \sim 0.8$.[42] The rapid decrease of $Q(T)$ indicates that self-heating is detrimental for operation of the coherent THz oscillator and ultimately limits its performance.[23] On the other hand, T dependence of the Swihart velocity facilitates a broad-range tuning of the resonance frequency, which may be beneficial for the oscillator.

Our analysis of T dependence of resonant voltages revealed that the effective penetration depth that determines the kinetic inductance and the speed of electromagnetic waves in intrinsic Josephson junctions, see Eq. (1), is exhibiting a flat T dependence at low T, resembling T dependence of the c-axis critical current. It is distinctly different from the linear T dependence of $\lambda_{ab}(T)$, obtained from surface impedance measurements.[12,13] We have argued that nontrivial physical phenomena, such as breakdown of the local London approximation at the atomic scale, are responsible for this distinct discrepancy, which deserves further theoretical consideration.

ACKNOWLEDGMENTS

We are grateful to A. Rydh and H. Motzkau for assistance in experiment and to the Swedish Research Council and the SU-Core Facility in Nanotechnology for financial and technical support, respectively.

[1] R. Kleiner, F. Steinmeyer, G. Kunkel, and P. Müller, Phys. Rev. Lett. **68**, 2394 (1992).
[2] J. C. Swihart, J. Appl. Phys. **32**, 461 (1961).
[3] M. J. Lancaster, F. Huang, A. Porch, B. Avenhaus, J. S. Hong, and D. Hung, IEEE Trans. Microwave Theor. Tech. **44**, 1339 (1996).
[4] P. V. Mason, J. Appl. Phys. **42**, 97 (1971).
[5] W. H. Henkels and C. J. Kircher, IEEE Trans. Magn. **13**, 63 (1977).
[6] I. M. Dmitrenko, I. K. Yanson, and V. M. Svistunov, JETP. Lett. **2**, 10 (1965).
[7] V. P. Koshelets and S. V. Shitov, Supercond. Sci. Technol. **13**, R53 (2000).
[8] H. B. Wang, S. Urayama, S. M. Kim, S. Arisawa, T. Hatano, and B. Y. Zhu, Appl. Phys. Lett. **89**, 252506 (2006).
[9] M. Cirillo, N. Grønbech-Jensen, M. R. Samuelsen, M. Salerno, and G. V. Rinati, Phys. Rev. B **58**, 12377 (1998).
[10] S. O. Katterwe, A. Rydh, H. Motzkau, A. B. Kulakov, and V. M. Krasnov, Phys. Rev. B **82**, 024517 (2010).
[11] K. L. Ngai, Phys. Rev. **182**, 555 (1969).
[12] D. A. Bonn, S. Kamal, K. Zhang, R. Liang, D. J. Baar, E. Klein, and W. N. Hardy, Phys. Rev. B **50**, 4051 (1994).
[13] T. Jacobs, S. Sridhar, Q. Li, G. D. Gu, and N. Koshizuka, Phys. Rev. Lett. **75**, 4516 (1995).

[14] A. Maeda, H. Kitano, and R. Inoue, J. Phys.: Condens. Matter **17**, R143 (2005).
[15] M. R. Trunin, J. Supercond. **11**, 381 (1998).
[16] V. M. Pan, A. A. Kalenyuk, A. L. Kasatkin, O. M. Ivanyuta, and G. A. Melkov, J. Supercond. Nov. Magn. **20**, 59 (2007).
[17] R. Prozorov and R. W. Giannetta, Supercond. Sci. Technol. **19**, R41 (2006).
[18] L. Ozyuzer, A. E. Koshelev, C. Kurter, N. Gopalsami, Q. Li, M. Tachiki, K. Kadowaki, T. Yamamoto, H. Minami, H. Yamaguchi, T. Tachiki, K. E. Gray, W. K. Kwok, and U. Welp, Science **318**, 1291 (2007).
[19] H. B. Wang, S. Guenon, J. Yuan, A. Iishi, S. Arisawa, T. Hatano, T. Yamashita, D. Koelle, and R. Kleiner, Phys. Rev. Lett. **102**, 017006 (2009).
[20] V. M. Krasnov, Phys. Rev. Lett. **103**, 227002 (2009).
[21] X. Hu and S. Z. Lin, Supercond. Sci. Technol. **23**, 053001 (2010).
[22] M. Tsujimoto, K. Yamaki, K. Deguchi, T. Yamamoto, T. Kashiwagi, H. Minami, M. Tachiki, K. Kadowaki, and R. A. Klemm, Phys. Rev. Lett. **105**, 037005 (2010).
[23] V. M. Krasnov, Phys. Rev. B **83**, 174517 (2011).
[24] V. M. Krasnov, Phys. Rev. B **82**, 134524 (2010).
[25] Note that Q may depend on N, for example, as a result of progressive self-heating, or varying matching between the internal resistance and the radiative impedance of the mesa. This destroys a simple $P_{\rm rad} \propto N^2$ dependence (Ref. 24).
[26] E. N. Economou, Phys. Rev. **182**, 539 (1969).
[27] R. Kleiner, Phys. Rev. B **50**, 6919 (1994).
[28] S. Sakai, A. V. Ustinov, H. Kohlstedt, A. Petraglia, and N. F. Pedersen, Phys. Rev. B **50**, 12905 (1994).
[29] S. Sakai, P. Bodin, and N. F. Pedersen, J. Appl. Phys. **73**, 2411 (1993).
[30] V. M. Krasnov, Phys. Rev. B **63**, 064519 (2001).
[31] S. O. Katterwe and V. M. Krasnov, Phys. Rev. B **80**, 020502(R) (2009).
[32] L. N. Bulaevskii, M. Zamora, D. Baeriswyl, H. Beck, and J. R. Clem, Phys. Rev. B **50**, 12831 (1994).
[33] A. Hosseini, S. Kamal, D. A. Bonn, R. Liang, and W. N. Hardy, Phys. Rev. Lett. **81**, 1298 (1998).
[34] A. Hosseini, D. M. Broun, D. E. Sheehy, T. P. Davis, M. Franz, W. N. Hardy, R. Liang, and D. A. Bonn, Phys. Rev. Lett. **93**, 107003 (2004).
[35] R. J. Radtke, V. N. Kostur, and K. Levin, Phys. Rev. B **53**, R522 (1996).
[36] V. M. Krasnov, H. Motzkau, T. Golod, A. Rydh, S. O. Katterwe, and A. B. Kulakov, Phys. Rev. B **84**, 054516 (2011).
[37] S. O. Katterwe, H. Motzkau, A. Rydh, and V. M. Krasnov, Phys. Rev. B **83**, 100510(R) (2011).
[38] S. O. Katterwe, A. Rydh, and V. M. Krasnov, Phys. Rev. Lett. **101**, 087003 (2008).
[39] D. W. McLaughlin and A. C. Scott, Phys. Rev. A **18**, 1652 (1978).
[40] Yu.I. Latyshev, A. E. Koshelev, V. N. Pavlenko, M. B. Gaifullin, T. Yamashita, and Y. Matsuda, Physica C **367**, 365 (2002).
[41] T. M. Benseman, A. E. Koshelev, K. E. Gray, W.-K. Kwok, U. Welp, K. Kadowaki, M. Tachiki, and T. Yamamoto, Phys. Rev. B **84**, 064523 (2011).
[42] V. M. Krasnov, T. Golod, T. Bauch, and P. Delsing, Phys. Rev. B **76**, 224517 (2007).
[43] M. B. Gaifullin, Y. Matsuda, N. Chikumoto, J. Shimoyama, K. Kishio, and R. Yoshizaki, Phys. Rev. Lett. **83**, 3928 (1999).
[44] R. G. Mints and I. B. Snapiro, Phys. Rev. B **51**, 3054 (1995).
[45] L. X. You, A. Yurgens, D. Winkler, M. Torstensson, S. Watauchi, and I. Tanaka, Supercond. Sci. Technol. **19**, S209 (2006).
[46] G. Hechtfischer, R. Kleiner, A. V. Ustinov, and P. Müller, Phys. Rev. Lett. **79**, 1365 (1997).
[47] M. H. Bae, H. J. Lee, and J. H. Choi, Phys. Rev. Lett. **98**, 027002 (2007).
[48] S. J. Kim, T. Hatano, and M. Blamire, J. Appl. Phys. **103**, 07C716 (2008).
[49] T. Bauch, T. Lindstrom, F. Tafuri, G. Rotoli, P. Delsing, T. Claeson, and F. Lombardi, Science **311**, 57 (2006).
[50] K. Inomata, S. Sato, K. Nakajima, A. Tanaka, Y. Takano, H. B. Wang, M. Nagao, H. Hatano, and S. Kawabata, Phys. Rev. Lett. **95**, 107005 (2005).
[51] K. Ota, K. Hamada, R. Takemura, M. Ohmaki, T. Machi, K. Tanabe, M. Suzuki, A. Maeda, and H. Kitano, Phys. Rev. B **79**, 134505 (2009).